Topological diagrammatic approach for charmed baryon decays

Hai-Yang Cheng[1,*], *Fanrong* Xu[2,**], and *Huiling* Zhong[2]

[1]Institute of Physics, Academia Sinica, Taipei, Taiwan 11529, Republic of China
[2]Department of Physics, Jinan University, Guangzhou 510632, People's Republic of China

Abstract. There exist two distinct ways in realizing the approximate SU(3) flavor symmetry of QCD to describe the two-body nonleptonic decays of charmed baryons, the irreducible SU(3) approach (IRA) and the topological diagram approach (TDA). The TDA has the advantage that it is more intuitive, graphic and easier to implement model calculations. We perform a global fit to the experimental data of two-body charmed baryon decays based on the TDA and discuss its equivalence with the IRA and their phenomenological implications.

1 Introduction

In the past few years, the experimental and theoretical progresses in the study of hadronic decays of charmed baryons are very impressive. On the experimental side, more than 35 measurements of branching fractions and decay asymmetries have been accumulated. On the theory aspect, there were many approaches developed in 1990s such as the relativistic quark model, the pole model and current algebra (for a review, see [1]). Besides the dynamical model calculations, a very promising approach is to use the approximate SU(3) flavor symmetry of QCD to describe the two-body nonleptonic decays of charmed baryons. There exist two distinct ways in realizing the flavor symmetry, the irreducible SU(3) approach (IRA) and the topological diagram approach (TDA). They provide a powerful tool for a model-independent analysis. Among them, the IRA has become very popular in the past few years. In the IRA, SU(3) tensor invariants are constructed through the short-distance effective Hamiltonian, while in the TDA, the topological diagrams are classified according to the topologies in the flavor flow of weak decay diagrams with all strong-interaction effects included implicitly.

Within the framework of the IRA, two-body nonleptonic decays of charmed baryons were first analyzed in Refs. [2, 3]. After 2014, this approach became rather popular. However, the early studies of the IRA have overlooked the fact that charmed baryon decays are governed by several different partial-wave amplitudes which have distinct kinematic and dynamic effects. In other words, S- and P-waves were not distinguished in the early analysis and the IRA amplitudes are fitted only to the measured rates. After the pioneer work in Ref. [4], it became a common practice to perform a global fit of both S- and P-wave parameters to the data of

*e-mail: phcheng@phys.sinica.edu.tw
**e-mail: fanrongxu@jnu.edu.cn

branching fractions and decay asymmetries [5–9]. Just like the case of hyperon decays, non-trivial relative strong phases between S- and P-wave amplitudes may exist, but they were usually not considered in realistic model calculations of the decay asymmetry α.

The first analysis of two-body nonleptonic decays of antitriplet charmed baryons $\mathcal{B}_c(\bar{3}) \to \mathcal{B}(8)M(8+1)$ within the framework of the TDA was performed by Kohara [10]. A subsequent study was given by Chau, Cheng and Tseng (CCT) in Ref. [11] followed by some recent analyses in the TDA [12–15]. Unlike the IRA, global fits to the rates and decay asymmetries in the TDA were not available until recently.

Although the TDA has been applied very successfully to charmed meson decays [16–18], its application to charmed baryon decays is more complicated than the IRA. As stressed in Ref. [12], it is easy to determine the independent amplitudes in the IRA, while the TDA gives some redundancy. Some of the amplitudes are not independent and therefore should be absorbed into other amplitudes. Nevertheless, the TDA has the advantage that it is more intuitive, graphic and easier to implement model calculations. The extracted topological amplitudes by fitting to available data will enable us to probe the relative importance of different underlying decay mechanisms, and to relate one process to another at the topological amplitude level.

2 TDA

Since baryons are made of three quarks in contrast to two quarks for the mesons, the application of TDA to the baryon case will inevitably lead to some complications, for example, the symmetry of the quarks in flavor space could be different. As shown explicitly in Ref. [19], physics is independent of the convention one chooses for the wave functions of the octet baryons. We prefer to use the bases $\psi^k(8)_{A_{12}}$ and $\psi^k(8)_{S_{12}}$ for octet baryons as they are orthogonal to each other:

$$\begin{aligned} |\psi^k(8)_{A_{12}}\rangle &= \sum_{q_a,q_b,q_c} |[q_a q_b]q_c\rangle\langle[q_a q_b]q_c|\psi^k(8)_{A_{12}}\rangle, \\ |\psi^k(8)_{S_{12}}\rangle &= \sum_{q_a,q_b,q_c} |\{q_a q_b\}q_c\rangle\langle\{q_a q_b\}q_c|\psi^k(8)_{S_{12}}\rangle, \end{aligned} \tag{1}$$

denoting the octet baryon states that are antisymmetric and symmetric in the first two quarks, respectively. Hence,

$$|\mathcal{B}^{m,k}(8)\rangle = a\,|\chi^m(1/2)_{A_{12}}\rangle|\psi^k(8)_{A_{12}}\rangle + b\,|\chi^m(1/2)_{S_{12}}\rangle|\psi^k(8)_{S_{12}}\rangle \tag{2}$$

with $|a|^2 + |b|^2 = 1$, where $\chi^m(1/2)_{A,S}$ are the spin parts of the wave function defined in Eq. (23) of Ref. [11].

In terms of the octet baryon wave functions given in Eq. (2), the relevant topological diagrams for the decays of antitriplet charmed baryons $\mathcal{B}_c(\bar{3}) \to \mathcal{B}(8)M(8+1)$ are depicted in Fig. 1: the external W-emission, T; the internal W-emission C; the inner W-emission C'; W-exchange diagrams E_{1A}, E_{1S}, E_{2A}, E_{2S}, E_3 and the hairpin diagram E_h. Since there are two possible penguin contractions, we will have penguin diagrams P_1, P_{2A}, P_{2S} as well as P'_1, P'_{2A}, P'_{2S}. The topologies P_h and P'_h are hairpin penguin diagrams. The decay amplitudes

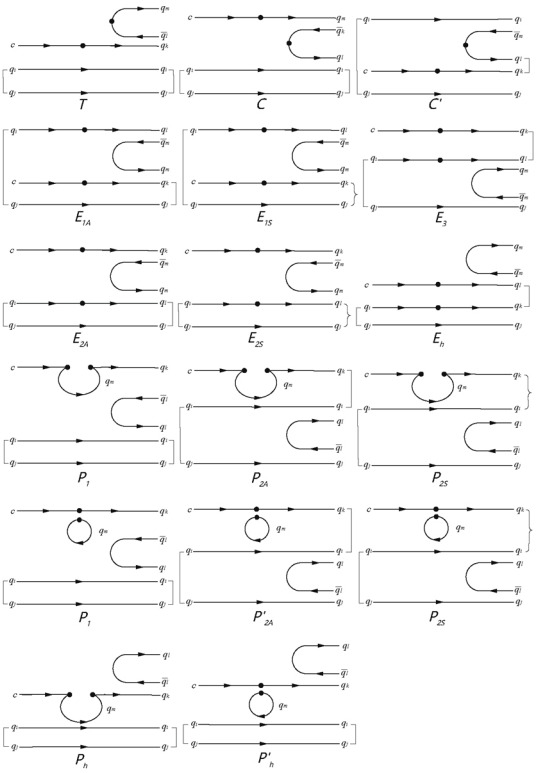

Figure 1: Topological diagrams contributing to $\mathcal{B}_c(\bar{3}) \to \mathcal{B}(8)M(8+1)$ decays.

of $\mathcal{B}_c(\bar{3}) \to \mathcal{B}(8)M(8+1)$ in the TDA have the expressions [20, 21]:

$$\begin{aligned}
\mathcal{A}_{\rm TDA} = \;& T(\mathcal{B}_c)^{ij}H_l^{km}(\mathcal{B}_8)_{ijk}(M^\dagger)_m^l \\
&+ C(\mathcal{B}_c)^{ij}H_k^{ml}(\mathcal{B}_8)_{ijl}(M)_m^k + C'(\mathcal{B}_c)^{ij}H_m^{kl}(\mathcal{B}_8)_{klj}(M)_i^m \\
&+ E_{1A}(\mathcal{B}_c)^{ij}H_i^{kl}(\mathcal{B}_8)_{jkm}(M)_l^m + E_{1S}(\mathcal{B}_c)^{ij}H_i^{kl}(M)_l^m\left[(\mathcal{B}_8)_{jmk} + (\mathcal{B}_8)_{kmj}\right] \\
&+ E_{2A}(\mathcal{B}_c)^{ij}H_i^{kl}(\mathcal{B}_8)_{jlm}(M)_k^m + E_{2S}(\mathcal{B}_c)^{ij}H_i^{kl}(M)_k^m\left[(\mathcal{B}_8)_{jml} + (\mathcal{B}_8)_{lmj}\right] \\
&+ E_3(\mathcal{B}_c)^{ij}H_i^{kl}(\mathcal{B}_8)_{klm}(M)_j^m + E_h(\mathcal{B}_c)^{ij}H_i^{kl}(\mathcal{B}_8)_{klj}(M)_m^m \\
&+ P_h(\mathcal{B}_c)^{ij}H_m^{mk}(\mathcal{B}_8)_{ijk}(M)_l^l + P_1(\mathcal{B}_c)^{ij}H_m^{mk}(\mathcal{B}_8)_{ijl}(M)_k^l \\
&+ P_{2A}(\mathcal{B}_c)^{ij}H_m^{mk}(\mathcal{B}_8)_{kil}(M)_j^l + P_{2S}(\mathcal{B}_c)^{ij}H_m^{mk}(M)_j^l\left[(\mathcal{B}_8)_{kli} + (\mathcal{B}_8)_{ilk}\right] \\
&+ P'_h(\mathcal{B}_c)^{ij}H_m^{km}(\mathcal{B}_8)_{ijk}(M)_l^l + P'_1(\mathcal{B}_c)^{ij}H_m^{km}(\mathcal{B}_8)_{ijl}(M)_k^l \\
&+ P'_{2A}(\mathcal{B}_c)^{ij}H_m^{km}(\mathcal{B}_8)_{kil}(M)_j^l + P'_{2S}(\mathcal{B}_c)^{ij}H_m^{km}(M)_j^l\left[(\mathcal{B}_8)_{kli} + (\mathcal{B}_8)_{ilk}\right],
\end{aligned} \tag{3}$$

where $(\mathcal{B}_c)^{ij}$ is an antisymmetric baryon matrix standing for antitriplet charmed baryons, $(\mathcal{B}_8)^i_j$ and M^i_j represent octet baryons and nonet mesons, respectively, and the tensor coefficient H_m^{kl} related to the CKM matrix elements appears in the standard model Hamiltonian with $H_m^{kl}(\bar{q}_k c)(\bar{q}_l q^m)$. The contraction of the two indices of H_m^{kl}, namely, H_m^{ml}, is induced in the penguin diagrams P_1, P_{2A}, P_{2S} and P_h, while H_l^{kl} in the penguin diagrams P'_1, P'_{2A}, P'_{2S} and P'_h.

In diagrams T and C, the two spectator quarks q_i and q_j are antisymmetric in flavor. Notice that the final-state quarks q_l and q_k in topological diagrams C', E_3 and E_h also must be antisymmetric in flavor owing to the Körner-Pati-Woo (KPW) theorem which states that the quark pair in a baryon produced by weak interactions is required to be antisymmetric in flavor in the SU(3) limit [22]. Likewise, the KPW theorem together with the pole model also leads to [23]

$$E_{2A} = -E_{1A}, \qquad E_{2S} = -E_{1S}. \tag{4}$$

As a result, the number of independent topological diagrams depicted in Fig. 1 and the TDA amplitudes in Eq. (3) is 7.

Working out Eq. (3) for $\mathcal{B}_c(\bar{3}) \to \mathcal{B}(8)M(8+1)$ decays, the obtained TDA decay amplitudes are listed in Tables I and II of Ref. [20]. Among the 7 TDA amplitudes given in Eq. (3), there still exist 2 redundant degrees of freedom through the redefinitions [11]:

$$\begin{aligned}
&\tilde{T} = T - E_{1S}, \quad \tilde{C} = C + E_{1S}, \quad \tilde{C}' = C' - 2E_{1S}, \\
&\tilde{E}_1 = E_{1A} + E_{1S} - E_3, \quad \tilde{E}_h = E_h + 2E_{1S}.
\end{aligned} \tag{5}$$

A closer look of the TDA amplitudes of Cabibbo-favored, singly-Cabibbo-suppressed and doubly-Cabibbo-suppresssed decays given in Tables I and II shows that E_{1S} can be absorbed by T, C, C', E_1 and E_h, as shown in the above equation. Hence, the redundant E_{1S} can be eliminated. Also the amplitude E_3 is always accompanied by $E_{1A} + E_{1S}$. Consequently, it can be absorbed by the combination of $E_{1A} + E_{1S}$. As a result, among the seven topological amplitudes T, C, C', E_{1A}, E_h, E_{1S} and E_3, the last two are redundant degrees of freedom and can be omitted through redefinitions. [1] It is clear that the minimum set of the topological amplitudes in TDA is 5. This is in agreement with the number of tensor invariants found in IRA [25].

It should be stressed that the redefinition given in Eq. (5) is not unique. another redefinition, for example,

$$\begin{aligned}
&\overline{T} = T - C'/2, \quad \overline{C} = C - C'/2, \quad \overline{E}_{1S} = E_{1S} - C'/2, \\
&\overline{E}_{1A} = E_{1A} - E_3 + C'/2, \quad \overline{E}_h = E_h + C',
\end{aligned} \tag{6}$$

also works.

2.1 Equivalence of TDA and IRA (I)

To demonstrate the equivalence between the TDA and IRA, we need to show that the number of the minimum set of tensor invariants in the IRA and the topological amplitudes in the TDA is the same. We follow Ref. [12] to write down the general SU(3) invariant decay amplitudes in the IRA:

$$\begin{aligned}
\mathcal{A}_{\rm IRAa} = \;& a_1 (\mathcal{B}_c)_i (H_6)^{ik}_j (\mathcal{B}_8)^j_k M^l_l + a_2 (\mathcal{B}_c)_i (H_6)^{ik}_j (\mathcal{B}_8)^l_k M^j_l + a_3 (\mathcal{B}_c)_i (H_6)^{ik}_j (\mathcal{B}_8)^j_l M^l_k \\
&+ a_4 (\mathcal{B}_c)_i (H_6)^{jk}_l (\mathcal{B}_8)^i_j M^l_k + a_5 (\mathcal{B}_c)_i (H_6)^{jk}_l (\mathcal{B}_8)^l_j M^i_k \\
&+ a_6 (\mathcal{B}_c)_i \left(H_{\overline{15}}\right)^{ik}_j (\mathcal{B}_8)^j_k M^l_l + a_7 (\mathcal{B}_c)_i \left(H_{\overline{15}}\right)^{ik}_j (\mathcal{B}_8)^l_k M^j_l \\
&+ a_8 (\mathcal{B}_c)_i \left(H_{\overline{15}}\right)^{ik}_j (\mathcal{B}_8)^j_l M^l_k + a_9 (\mathcal{B}_c)_i \left(H_{\overline{15}}\right)^{jk}_l (\mathcal{B}_8)^i_j M^l_k \\
&+ a_{10} (\mathcal{B}_c)_i \left(H_{\overline{15}}\right)^{jk}_l (\mathcal{B}_8)^l_j M^i_k.
\end{aligned} \tag{7}$$

[1] It was claimed in a recent work [24] that the relations of $T = C$ and $E_1 = E_2$ (or $T_1 = T_2$ and $T_4 = T_5$ in the notation of Ref. [24]) can be used to reduce the number of independent degrees of freedom from 7 to 5. Since the color-allowed T and the color-suppressed C are different topologies, the relation of $T = C$ does not hold and likewise for E_1 and E_2.

For the explicit expressions of $(H_6)^{ij}_k$ and $\left(H_{\overline{15}}\right)^{ij}_k$, see Ref. [12]. The first five terms associated with H_6 are not totally independent as one of them is redundant through the redefinition. It should be stressed that the redefinition is not unique. For example, we will consider the following redefinitions

$$a'_1 = a_1 - a_5, \quad a'_2 = a_2 + a_5, \quad a'_3 = a_3 + a_5, \quad a'_4 = a_4 + a_5, \tag{8}$$

and [12]

$$a''_1 = a_1 + a_2, \quad a''_2 = a_2 - a_3, \quad a''_3 = a_3 - a_4, \quad a''_5 = a_5 + a_3. \tag{9}$$

As for the five terms associated with $H_{\overline{15}}$ in Eq. (16), four of them are prohibited by the KPW theorem and the pole model, namely, $a_6 = a_7 = a_8 = a_{10} = 0$ [23, 25].

By comparing the TDA amplitudes in Tables 1 and 2 of [20] with the IRA amplitudes given in Tables 14-16 of Ref. [12], we arrive at the relations

$$\begin{aligned} &\tilde{T} = \frac{1}{2}(-a_2 + a_4 + a_9), \qquad \tilde{C} = \frac{1}{2}(a_2 - a_4 + a_9), \\ &\tilde{C}' = -a_2 - a_5, \qquad \tilde{E}_1 = a_3 + a_5, \qquad \tilde{E}_h = -a_1 + a_5. \end{aligned} \tag{10}$$

Therefore, we have the correspondence

$$\begin{aligned} &\tilde{T} = \frac{1}{2}(-a'_2 + a'_4 + a'_9), \qquad \tilde{C} = \frac{1}{2}(a'_2 - a'_4 + a'_9), \\ &\tilde{C}' = -a'_2, \qquad \tilde{E}_1 = a'_3, \qquad \tilde{E}_h = -a'_1. \end{aligned} \tag{11}$$

in terms of the redefinitions given in Eq. (8). The equivalence between the TDA and IRA is thus established.

There is another set of the IRA amplitudes given in Ref. [25]

$$\begin{aligned} \mathcal{A}_{\rm IRAb} = \; & \tilde{f}^a\,(\mathcal{B}_c)^{ik}\,(H_6)_{ij}\,(\mathcal{B}_8)^j_k\,M^l_l + \tilde{f}^b\,(\mathcal{B}_c)^{ik}\,(H_6)_{ij}\,(\mathcal{B}_8)^l_k\,M^j_l + \tilde{f}^c\,(\mathcal{B}_c)^{ik}\,(H_6)_{ij}\,(\mathcal{B}_8)^j_l\,M^l_k \\ & + \tilde{f}^d\,(\mathcal{B}_c)^{kl}\,(H_6)_{ij}\,(\mathcal{B}_8)^i_k\,M^j_l + \tilde{f}^e\,(\mathcal{B}_c)_j\left(H_{\overline{15}}\right)^{ik}_l\,(\mathcal{B}_8)^j_i\,M^l_k. \end{aligned} \tag{12}$$

The equivalence between $\widetilde{\rm TDA}$, IRAa and IRAb leads to the relations:

$$\begin{aligned} &\tilde{T} = \frac{1}{2}(\tilde{f}^b + \tilde{f}^e), \qquad \tilde{C} = \frac{1}{2}(-\tilde{f}^b + \tilde{f}^e), \\ &\tilde{C}' = \tilde{f}^b - \tilde{f}^d, \qquad \tilde{E}_1 = -\tilde{f}^c, \qquad \tilde{E}_h = \tilde{f}^a, \end{aligned} \tag{13}$$

2.2 Equivalence of TDA and IRA (II)

In Refs. [20, 21] the equivalence of TDA with IRA is established by first writing down the TDA and IRA amplitudes of $\mathcal{B}_c(\bar{3}) \to \mathcal{B}(8)M(8+1)$ decays and then comparing them to figure out their relations. Here we will make a direct transformation from TDA to IRA and show that they are identical.

In terms of $(\mathcal{B}_c)_i$ and $(\mathcal{B}_8)^i_j$ defined by $(\mathcal{B}_c)^{ij} = \epsilon^{ijk}(\mathcal{B}_c)_k$ and $(\mathcal{B}_8)_{ijk} = \epsilon_{ijl}(\mathcal{B}_8)^l_k$, respectively, Eq. (3) can be recast to

$$\begin{aligned} \mathcal{A}_{\rm TDA} = \; & (2T - C' - 2E_{1S})(\mathcal{B}_c)_i(\mathcal{B}_8)^i_j H^{jl}_m M^m_l + (2C + C' - 2E_{2S})(\mathcal{B}_c)_i(\mathcal{B}_8)^i_j H^{lj}_m M^m_l \\ & + C'(\mathcal{B}_c)_i(\mathcal{B}_8)^l_j(H^{ji}_m - H^{ij}_m)M^m_l + (E_{1A} - E_{1S} - E_3)(\mathcal{B}_c)_i(\mathcal{B}_8)^j_m H^{il}_j M^m_l \\ & + (E_{2A} - E_{2S} + E_3)(\mathcal{B}_c)_i(\mathcal{B}_8)^j_m H^{li}_j M^m_l - E_h(\mathcal{B}_c)_i(\mathcal{B}_8)^l_j(H^{ij}_l - H^{ji}_l)M^m_m \\ & + 2E_{1S}(\mathcal{B}_c)_i(\mathcal{B}_8)^m_j H^{jl}_m M^i_l + 2E_{2S}(\mathcal{B}_c)_i(\mathcal{B}_8)^m_j H^{lj}_m M^i_l + \cdots, \end{aligned} \tag{14}$$

where only the non-penguin terms are kept. Substituting the relation

$$H_k^{ij} = \frac{1}{2}\left[H(\overline{15})_k^{ij} + H(6)_k^{ij}\right] + \cdots \tag{15}$$

into the above equation yields

$$\begin{aligned}\mathcal{A}_{\rm TDA} = \;& (T+C)(\mathcal{B}_c)_i \left(H_{\overline{15}}\right)_m^{jl} (\mathcal{B}_8)_j^i M_l^m - E_h(\mathcal{B}_c)_i\,(H_6)_l^{ij}\,(\mathcal{B}_8)_j^l M_m^m \\ & + (T-C-C'-2E_{1S})(\mathcal{B}_c)_i\,(H_6)_m^{jl}\,(\mathcal{B}_8)_j^i M_l^m - C'(\mathcal{B}_c)_i\,(H_6)_m^{ij}\,(\mathcal{B}_8)_j^l M_l^m \\ & + (E_{1A}-E_{1S}-E_3)(\mathcal{B}_c)_i\,(H_6)_j^{il}\,(\mathcal{B}_8)_m^j M_l^m + 2E_{1S}(\mathcal{B}_c)_i\,(H_6)_m^{jl}\,(\mathcal{B}_8)_j^m M_l^i\end{aligned} \tag{16}$$

Comparing the TDA amplitudes with the IRA ones in Eq. (16), we obtain

$$\begin{aligned} &a_1 = -E_h, \qquad a_2 = -C', \qquad a_3 = E_{1A} - E_{1S} - E_3, \\ &a_4 = T - C - C' - 2E_{1S}, \qquad a_5 = 2E_{1S}, \qquad a_9 = T + C.\end{aligned} \tag{17}$$

These lead to

$$\begin{aligned} &a_1' = a_1 - a_5 = -\tilde{E}_h, \qquad a_2' = a_2 + a_5 = -\tilde{C}', \\ &a_3' = a_3 + a_5 = \tilde{E}_1, \qquad a_4' = a_4 + a_5 = \tilde{T} - \tilde{C} - \tilde{C}', \\ &a_9 = \tilde{T} + \tilde{C}, \qquad a_6 = a_7 = a_8 = a_{10} = 0,\end{aligned} \tag{18}$$

consistent with Eq. (34) of Ref. [20]. Also, we have

$$\begin{aligned} &a_1'' = a_1 - a_2 = -\overline{E}_h, \qquad a_2'' = a_2 - a_3 = -\overline{E}_{1A} + \overline{E}_{1S} \\ &a_3'' = a_3 - a_4 = -\overline{T} + \overline{C} + \overline{E}_{1A} + \overline{E}_{1S}, \qquad a_5'' = a_3 + a_5 = \overline{E}_{1A} + \overline{E}_{1S}, \\ &a_9 = \overline{T} + \overline{C}, \qquad a_6 = a_7 = a_8 = a_{10} = 0,\end{aligned} \tag{19}$$

3 Numerical Analysis and Results

As there are 5 independent tilde TDA amplitudes given in Eq. (5), we have totally 19 unknown parameters to describe the magnitudes and the phases of the respective S- and P-wave amplitudes, namely,

$$\begin{aligned} &|\tilde{T}|_S e^{i\delta_S^{\tilde{T}}}, \quad |\tilde{C}|_S e^{i\delta_S^{\tilde{C}}}, \quad |\tilde{C}'|_S e^{i\delta_S^{\tilde{C}'}}, \quad |\tilde{E}_1|_S e^{i\delta_S^{\tilde{E}_1}}, \quad |\tilde{E}_h|_S e^{i\delta_S^{\tilde{E}_h}}, \\ &|\tilde{T}|_P e^{i\delta_P^{\tilde{T}}}, \quad |\tilde{C}|_P e^{i\delta_P^{\tilde{C}}}, \quad |\tilde{C}'|_P e^{i\delta_P^{\tilde{C}'}}, \quad |\tilde{E}_1|_P e^{i\delta_P^{\tilde{E}_1}}, \quad |\tilde{E}_h|_P e^{i\delta_P^{\tilde{E}_h}}, \end{aligned} \tag{20}$$

collectively denoted by $|X_i|_S e^{i\delta_S^{X_i}}$ and $|X_i|_P e^{i\delta_P^{X_i}}$, where the subscripts S and P denote the S- and P-wave components of each TDA amplitude. Since there is an overall phase which can be omitted, we shall set $\delta_S^{\tilde{T}} = 0$. Likewise, for the tidle IRA amplitudes given in Eq. (12), we also have

$$\begin{aligned} &|\tilde{f}^a|_S e^{i\delta_S^{\tilde{f}a}}, \quad |\tilde{f}^b|_S e^{i\delta_S^{\tilde{f}b}}, \quad |\tilde{f}^c|_S e^{i\delta_S^{\tilde{f}c}}, \quad |\tilde{f}^d|_S e^{i\delta_S^{\tilde{f}d}}, \quad |\tilde{f}^e|_S e^{i\delta_S^{\tilde{f}e}}, \\ &|\tilde{f}^a|_P e^{i\delta_P^{\tilde{f}a}}, \quad |\tilde{f}^b|_P e^{i\delta_P^{\tilde{f}b}}, \quad |\tilde{f}^c|_P e^{i\delta_P^{\tilde{f}c}}, \quad |\tilde{f}^d|_P e^{i\delta_P^{\tilde{f}d}}, \quad |\tilde{f}^e|_P e^{i\delta_P^{\tilde{f}e}}. \end{aligned} \tag{21}$$

We shall aslo set $\delta_S^{\tilde{f}a} = 0$. Of course, physics is independent of which phase is removed. Hence, in both cases we are left with 19 parameters.

In terms of the S- and P-wave amplitudes given in

$$M(\mathcal{B}_c \to \mathcal{B}_f + P) = i\bar{u}_f(A - B\gamma_5)u_c, \tag{22}$$

and their phases δ_S and δ_P, respectively, the decay rate and Lee-Yang parameters read

$$\Gamma = \frac{p_c}{8\pi}\frac{(m_i+m_f)^2-m_P^2}{m_i^2}\left(|A|^2+\kappa^2|B|^2\right),$$
$$\alpha = \frac{2\kappa|A^*B|\cos(\delta_P-\delta_S)}{|A|^2+\kappa^2|B|^2},\quad \beta = \frac{2\kappa|A^*B|\sin(\delta_P-\delta_S)}{|A|^2+\kappa^2|B|^2},\quad \gamma = \frac{|A|^2-\kappa^2|B|^2}{|A|^2+\kappa^2|B|^2}, \tag{23}$$

where $\kappa = p_c/(E_f+m_f) = \sqrt{(E_f-m_f)/(E_f+m_f)}$ and $\alpha^2+\beta^2+\gamma^2 = 1$. It is clear that the magnitudes of S- and P-wave amplitudes can be determined from Γ and γ. As for the phase shift between S- and P-wave amplitudes, it is naively expected that $\delta_P-\delta_S = \arctan(\beta/\alpha)$ (see, for example, Ref. [26]). However, this is is somewhat misleading as the range of this solution is limited to $(-\frac{\pi}{2},\frac{\pi}{2})$, which does not fully cover the phase-shift space. The correct one is [20]

$$\delta_P-\delta_S = 2\arctan\frac{\beta}{\sqrt{\alpha^2+\beta^2}+\alpha}. \tag{24}$$

This naturally covers the correct solution space without imposing manual modification. As an example, consider the recent LHCb measurements of the decay parameters $\alpha = -0.782\pm 0.010$ and $\beta = 0.368\pm 0.017$ for the decay $\Lambda_c^+\to\Lambda\pi^+$. The formula $\delta_P-\delta_S = \arctan(\beta/\alpha)$ yields $\delta_P-\delta_S = -0.44$ rad, while Eq. (24) leads to $\delta_P-\delta_S = 2.70$ rad.

As noticed in Ref. [25], there is a so-called Z_2 ambiguity in the determination of phases, namely, $(\delta_S^{X_i},\delta_P^{X_i})\to(-\delta_S^{X_i},-\delta_P^{X_i})$. Since β is proportional to $\sin(\delta_P-\delta_S)$, this sign ambiguity can be resolved by the measurement of β as just noticed in passing. The sign of the Lee-Yang parameter γ depends on the relative magnitude of S- and P-wave amplitudes. Hence we also need measurements of γ to select the solution for $|A|$ and $|B|$. Recently, LHCb has performed the first measurements of all the Lee-Yang parameters in $\Lambda_c^+\to\Lambda\pi^+$ and $\Lambda_c^+\to\Lambda K^+$; see Table 1.

Table 1: LHCb measurements of the decay parameters for $\Lambda_c^+\to\Lambda\pi^+$ $\Lambda_c^+\to\Lambda K^+$ and $\Lambda_c^+\to pK_S^0$ decays [27].

Decay	α	β	γ
$\Lambda_c^+\to\Lambda\pi^+$	$-0.782\pm0.009\pm0.004$	$0.368\pm0.019\pm0.008$	$0.502\pm0.016\pm0.006$
$\Lambda_c^+\to\Lambda K^+$	$-0.569\pm0.059\pm0.028$	$0.35\pm0.12\pm0.04$	$-0.743\pm0.067\pm0.024$
$\Lambda_c^+\to pK_S^0$	$-0.744\pm0.012\pm0.009$	–	–

Fitted tilde TDA and IRA amplitudes collectively denoted by X_i are shown in Table 2, where we have used the LHCb data in Table 1 and the data collected in Table VII of Ref. [20]. We have set $\delta_S^{\tilde{T}} = 0$ and $\delta_S^{\tilde{f}^a} = 0$. The fit results based on the tilde TDA and tilde IRA are shown in Table 3. In the following we discuss their implications.

For the decay $\Lambda_c^+\to\Xi^0K^+$, BESIII found [26]

$$\alpha = 0.01\pm0.16\pm0.03,\quad \beta = -0.64\pm0.69\pm0.13,\quad \gamma = -0.77\pm0.58\pm0.11, \tag{25}$$

and uncovered two sets of solutions for the magnitudes of S- and P-wave amplitudes in units of $10^{-2}G_F\,\mathrm{GeV}^2$:

$$\text{I.}\begin{cases}|A| = 1.6^{+1.9}_{-1.6}\pm0.4,\\ |B| = 18.3\pm2.8\pm0.7,\end{cases}\qquad \text{II.}\begin{cases}|A| = 4.3^{+0.7}_{-0.2}\pm0.4,\\ |B| = 6.7^{+8.3}_{-6.7}\pm1.6,\end{cases} \tag{26}$$

Table 2: Fitted tilde TDA and IRA amplitudes collectively denoted by X_i. We have set $\delta_S^{\tilde{T}} = 0$ and $\delta_S^{\tilde{f}^a} = 0$.

	$\lvert X_i\rvert_S$	$\lvert X_i\rvert_P$	$\delta_S^{X_i}$	$\delta_P^{X_i}$
	($10^{-2}G_F$ GeV^2)		(in radian)	
$\tilde{T}$	4.23 ± 0.12	12.47 ± 0.31	–	2.41 ± 0.04
$\tilde{C}$	2.94 ± 0.52	11.76 ± 0.92	3.03 ± 0.11	-0.72 ± 0.18
$\tilde{C}'$	5.38 ± 0.44	19.03 ± 0.86	-0.04 ± 0.06	2.23 ± 0.12
$\tilde{E}_1$	2.90 ± 0.20	10.10 ± 0.50	-2.81 ± 0.06	1.88 ± 0.10
$\tilde{E}_h$	3.88 ± 0.77	13.43 ± 1.92	2.65 ± 0.13	-1.94 ± 0.21
$\tilde{f}^a$	4.31 ± 0.68	15.78 ± 2.23	–	1.73 ± 0.12
$\tilde{f}^b$	7.10 ± 0.72	24.40 ± 1.04	-2.73 ± 0.10	-0.27 ± 0.13
$\tilde{f}^c$	2.92 ± 0.19	10.17 ± 0.48	-2.34 ± 0.11	2.32 ± 0.13
$\tilde{f}^d$	1.57 ± 0.62	7.24 ± 2.20	-2.80 ± 0.22	0.31 ± 0.24
$\tilde{f}^e$	1.47 ± 0.67	0.69 ± 1.11	-2.46 ± 0.20	-1.29 ± 2.50

as well as two solutions for the phase shift,

$$\delta_P - \delta_S = -1.55 \pm 0.25 \pm 0.05 \ \text{ or } \ 1.59 \pm 0.25 \pm 0.05 \ \text{rad}. \tag{27}$$

Our fits with $|A| = 2.75 \pm 0.19$, $|B| = 9.59 \pm 0.47$, $\alpha_{\Xi^0K^+} = -0.03 \pm 0.12$, $\beta_{\Xi^0K^+} = -0.98 \pm 0.02$ and $\delta_P - \delta_S = -1.60 \pm 0.12$ rad are consistent with the first phase-shift solution as well as the Lee-Yang parameters $\alpha_{\Xi^0K^+}$ and $\beta_{\Xi^0K^+}$. However, our result of $\mathcal{B}(\Lambda_c^+ \to \Xi^0K^+) = (0.33 \pm 0.03)\%$ is smaller than the measured value of $(0.55 \pm 0.07)\%$ [28].

It should be stressed that although the BESIII's measurement of $\alpha_{\Xi^0K^+}$ is in good agreement with zero, it does not mean that the theoretical predictions in the 1990s with vanishing or very small S-wave amplitude are confirmed. We have checked that if we set $\delta_S^{X_i} = \delta_P^{X_i} = 0$ from the outset and remove the input of $(\alpha_{\Xi^0K^+})_{\rm exp}$, the fit $\alpha_{\Xi^0K^+}$ will be of order 0.95 . Hence, we conclude that it is necessary to incorporate the phase shifts to accommodate the data. It is the smallness of $|\cos(\delta_P - \delta_S)| \sim 0.02$ that accounts for the nearly vanishing $\alpha_{\Xi^0K^+}$.

Besides the decay $\Lambda_c^+ \to \Xi^0K^+$, we have noticed that the following modes $\Xi_c^0 \to \Sigma^+K^-, \Sigma^+\pi^-, pK^-, p\pi^-, n\pi^0$ and $\Xi_c^+ \to p\pi^0, n\pi^+$ also receive contributions only from the topological W-exchange amplitude $\tilde{E}_1$. In the absence of strong phases in S- and P-wave amplitudes, they are expected to have large decay asymmetries. For example, $\alpha_{\Xi_c^0\to\Sigma^+K^-}$ was found to be $0.79^{+0.32}_{-0.33}$, 0.81 ± 0.16 and 0.98 ± 0.20, respectively, in Refs. [4–6]. Once the phase shifts are incorporated in the fit, the above-mentioned modes should have $\delta_P - \delta_S$ similar to that in $\Lambda_c^+ \to \Xi^0K^+$ and their decay asymmetries will become smaller (see Tables 3). In particular, for the CF channel $\Xi_c^0 \to \Sigma^+K^-$ whose branching fraction has been measured before, we predict that $\alpha_{\Xi_c^0\to\Sigma^+K^-} = -0.03 \pm 0.12$ similar to that of $\Lambda_c^+ \to \Xi^0K^+$. This can be used to test our theoretical framework.

The predicted $\mathcal{B}(\Xi_c^0 \to \Xi^-\pi^+) = (2.96 \pm 0.10)\%$ is noticeably higher than the measured value of $(1.80 \pm 0.52)\%$ by Belle [29], but it is in a good agreement with the sum rule derived in both TDA and IRA, namely,

$$\frac{\tau_{\Lambda_c^+}}{\tau_{\Xi_c^0}}\mathcal{B}(\Xi_c^0 \to \Xi^-\pi^+) = 3\mathcal{B}(\Lambda_c^+ \to \Lambda\pi^+) + \mathcal{B}(\Lambda_c^+ \to \Sigma^0\pi^+) - \frac{1}{\sin^2\theta_C}\mathcal{B}(\Lambda_c^+ \to n\pi^+). \tag{28}$$

Table 3: The fit results based on the tilde TDA (upper) and tilde IRA (lower). S- and P-wave amplitudes are in units of $10^{-2}G_F$ GeV^2 and $\delta_P - \delta_S$ in radian.

Channel	$10^2\mathcal{B}$	α	β	γ	$\lvert A\rvert$	$\lvert B\rvert$	$\delta_P - \delta_S$	$\mathcal{B}_{\rm exp}$	$\alpha_{\rm exp}$
$\Lambda_c^+ \to \Lambda^0\pi^+$	1.29 ± 0.05	-0.77 ± 0.01	0.38 ± 0.02	0.51 ± 0.01	5.55 ± 0.10	9.29 ± 0.21	2.68 ± 0.02	1.29 ± 0.05	-0.771 ± 0.011
	1.29 ± 0.05	-0.77 ± 0.01	0.38 ± 0.02	0.51 ± 0.01	5.55 ± 0.10	9.28 ± 0.21	2.68 ± 0.02		
$\Lambda_c^+ \to \Sigma^0\pi^+$	1.26 ± 0.05	-0.48 ± 0.02	0.34 ± 0.11	-0.81 ± 0.05	1.94 ± 0.24	19.29 ± 0.46	2.53 ± 0.15	1.27 ± 0.06	-0.47 ± 0.03
	1.26 ± 0.05	-0.48 ± 0.02	0.37 ± 0.10	-0.80 ± 0.05	2.02 ± 0.25	19.18 ± 0.47	2.48 ± 0.14		
$\Lambda_c^+ \to \Sigma^+\pi^0$	1.28 ± 0.05	-0.48 ± 0.02	0.34 ± 0.11	-0.81 ± 0.05	1.94 ± 0.24	19.29 ± 0.46	2.53 ± 0.15	1.25 ± 0.09	-0.49 ± 0.03
	1.27 ± 0.05	-0.48 ± 0.02	0.37 ± 0.10	-0.80 ± 0.05	2.02 ± 0.25	19.18 ± 0.47	2.48 ± 0.14		
$\Lambda_c^+ \to \Sigma^+\eta$	0.34 ± 0.03	-0.92 ± 0.04	0.03 ± 0.14	0.40 ± 0.10	2.97 ± 0.19	7.02 ± 0.68	3.11 ± 0.16	0.32 ± 0.04	-0.99 ± 0.06
	0.33 ± 0.03	-0.92 ± 0.04	-0.10 ± 0.16	0.37 ± 0.12	2.90 ± 0.19	7.12 ± 0.77	-3.04 ± 0.17		
$\Lambda_c^+ \to \Sigma^+\eta'$	0.35 ± 0.10	-0.44 ± 0.07	0.89 ± 0.06	0.12 ± 0.37	3.78 ± 1.14	20.99 ± 2.58	2.03 ± 0.08	0.44 ± 0.15	-0.46 ± 0.07
	0.46 ± 0.12	-0.44 ± 0.07	0.89 ± 0.05	0.09 ± 0.31	4.25 ± 1.05	24.19 ± 3.16	2.03 ± 0.08		
$\Lambda_c^+ \to \Xi^0 K^+$	0.33 ± 0.03	-0.03 ± 0.12	-0.98 ± 0.02	0.20 ± 0.09	2.75 ± 0.19	9.59 ± 0.47	-1.60 ± 0.12	0.55 ± 0.07	0.01 ± 0.16
	0.34 ± 0.03	-0.05 ± 0.11	-0.98 ± 0.02	0.20 ± 0.09	2.77 ± 0.18	9.66 ± 0.46	-1.62 ± 0.11		
$\Lambda_c^+ \to \Lambda^0 K^+$	0.0625 ± 0.0030	-0.57 ± 0.04	0.40 ± 0.07	-0.72 ± 0.04	0.56 ± 0.04	4.38 ± 0.11	2.54 ± 0.10	0.0635 ± 0.0031	-0.579 ± 0.041
	0.0627 ± 0.0030	-0.58 ± 0.04	0.39 ± 0.07	-0.72 ± 0.04	0.56 ± 0.04	4.39 ± 0.11	2.55 ± 0.10		
$\Lambda_c^+ \to \Sigma^0 K^+$	0.0384 ± 0.0029	-0.65 ± 0.08	0.76 ± 0.07	0.00 ± 0.11	0.83 ± 0.07	2.95 ± 0.13	2.27 ± 0.10	0.0382 ± 0.0051	-0.55 ± 0.20
	0.0390 ± 0.0027	-0.62 ± 0.07	0.79 ± 0.05	0.04 ± 0.11	0.86 ± 0.07	2.90 ± 0.14	2.23 ± 0.09		
$\Lambda_c^+ \to \Sigma^+ K_S$	0.0385 ± 0.0029	-0.65 ± 0.08	-0.76 ± 0.07	0.00 ± 0.11	0.83 ± 0.07	2.95 ± 0.13	2.27 ± 0.10	0.047 ± 0.014	
	0.0390 ± 0.0027	-0.62 ± 0.07	0.79 ± 0.05	0.04 ± 0.11	0.86 ± 0.07	2.90 ± 0.14	2.23 ± 0.09		
$\Lambda_c^+ \to n\pi^+$	0.072 ± 0.008	-0.53 ± 0.11	-0.71 ± 0.04	0.45 ± 0.11	1.30 ± 0.07	1.92 ± 0.25	-2.21 ± 0.12	0.066 ± 0.013	
	0.072 ± 0.007	-0.56 ± 0.10	-0.71 ± 0.04	0.42 ± 0.10	1.28 ± 0.07	1.96 ± 0.22	-2.24 ± 0.10		
$\Lambda_c^+ \to p\pi^0$	0.0196 ± 0.0036	-0.45 ± 0.31	-0.87 ± 0.28	-0.20 ± 0.54	0.50 ± 0.15	1.48 ± 0.42	-2.05 ± 0.41	$0.0156^{+0.0075}_{-0.0061}$	
	0.0200 ± 0.0040	-0.52 ± 0.12	-0.77 ± 0.35	-0.37 ± 0.63	0.45 ± 0.20	1.59 ± 0.48	-2.16 ± 0.29		
$\Lambda_c^+ \to pK_S$	1.55 ± 0.06	-0.74 ± 0.01	0.51 ± 0.18	-0.43 ± 0.21	3.97 ± 0.73	16.00 ± 1.31	2.54 ± 0.17	1.59 ± 0.07	-0.743 ± 0.015
	1.58 ± 0.06	-0.74 ± 0.01	0.47 ± 0.25	-0.47 ± 0.25	3.84 ± 0.91	16.36 ± 1.45	2.58 ± 0.24		
$\Lambda_c^+ \to p\eta$	0.153 ± 0.007	-0.65 ± 0.05	0.38 ± 0.26	-0.66 ± 0.16	0.98 ± 0.24	5.55 ± 0.28	2.61 ± 0.29	0.149 ± 0.008	
	0.150 ± 0.007	-0.67 ± 0.06	0.30 ± 0.43	-0.68 ± 0.21	0.93 ± 0.31	5.54 ± 0.36	2.72 ± 0.53		
$\Lambda_c^+ \to p\eta'$	0.053 ± 0.008	-0.43 ± 0.11	0.64 ± 0.25	-0.64 ± 0.24	0.70 ± 0.23	4.87 ± 0.57	2.17 ± 0.24	0.049 ± 0.009	
	0.051 ± 0.008	-0.40 ± 0.23	0.69 ± 0.24	-0.60 ± 0.23	0.73 ± 0.21	4.75 ± 0.55	2.10 ± 0.35		
$\Xi_c^0 \to \Xi^-\pi^+$	2.96 ± 0.10	-0.74 ± 0.03	0.67 ± 0.03	0.12 ± 0.04	8.03 ± 0.23	23.70 ± 0.58	2.41 ± 0.04	1.80 ± 0.52	-0.64 ± 0.05
	2.97 ± 0.10	-0.73 ± 0.03	0.67 ± 0.03	0.13 ± 0.04	8.10 ± 0.23	23.54 ± 0.58	2.39 ± 0.04		
$\Xi_c^+ \to \Xi^0\pi^+$	0.97 ± 0.16	-0.89 ± 0.08	0.29 ± 0.11	0.36 ± 0.14	2.93 ± 0.27	6.67 ± 0.96	2.83 ± 0.13	1.6 ± 0.8	
	0.95 ± 0.13	-0.91 ± 0.06	0.28 ± 0.10	0.30 ± 0.13	2.84 ± 0.25	6.90 ± 0.81	2.85 ± 0.11		
Channel	$10^2\mathcal{R}_X$	α	β	γ	$\lvert A\rvert$	$\lvert B\rvert$	$\delta_P - \delta_S$	$10^2(\mathcal{R}_X)_{\rm exp}$	$\alpha_{\rm exp}$
$\Xi_c^0 \to \Xi^- K^+$	4.38 ± 0.02	-0.73 ± 0.03	0.66 ± 0.03	0.20 ± 0.04	1.85 ± 0.05	5.46 ± 0.13	2.41 ± 0.04	2.75 ± 0.57	
	4.39 ± 0.02	-0.72 ± 0.03	0.66 ± 0.02	0.22 ± 0.04	1.86 ± 0.05	5.42 ± 0.13	2.39 ± 0.04		
$\Xi_c^0 \to \Lambda K_S^0$	23.1 ± 0.9	-0.61 ± 0.02	0.50 ± 0.13	-0.61 ± 0.11	2.38 ± 0.34	14.18 ± 0.47	2.46 ± 0.12	22.9 ± 1.4	
	23.1 ± 0.8	-0.61 ± 0.02	0.49 ± 0.17	-0.62 ± 0.13	2.37 ± 0.41	14.22 ± 0.49	2.47 ± 0.17		
$\Xi_c^0 \to \Sigma^0 K_S^0$	3.8 ± 0.6	-0.54 ± 0.38	-0.90 ± 0.11	0.18 ± 0.60	1.68 ± 0.49	4.33 ± 1.52	-2.15 ± 0.39	3.8 ± 0.7	
	3.7 ± 0.6	-0.64 ± 0.19	-0.86 ± 0.17	-0.01 ± 0.77	1.53 ± 0.65	4.76 ± 1.71	-2.26 ± 0.26		
$\Xi_c^0 \to \Sigma^+ K^-$	13.7 ± 0.9	-0.03 ± 0.12	-0.99 ± 0.01	-0.13 ± 0.09	2.75 ± 0.19	9.59 ± 0.47	-1.60 ± 0.12	12.3 ± 1.2	
	13.8 ± 0.9	-0.05 ± 0.11	-0.99 ± 0.01	-0.13 ± 0.09	2.77 ± 0.18	9.66 ± 0.46	-1.62 ± 0.11		

This sum rule was first derived in Ref. [25]. It is very useful to constrain the branching fraction of $\Xi_c^0 \to \Xi^-\pi^+$. This needs to be tested in the near future.

4 CP violation

The existence of strong phases in the partial-wave amplitudes of hadronic charmed baryon decays plays a pivotal role in a further exploration of CP violation in the charmed baryon sector. According to the standard model, CP violation is at a very small level in the decays of charmed hadrons. This is because of the relation of the CKM matrix elements, $\lambda_s \approx -\lambda_d$ with $\lambda_p \equiv V_{cp}^* V_{up}$. As a consequence, CP violation in the charm sector is usually governed by λ_b which is very tiny compared to λ_d or λ_s in magnitude. This also indicates that the corresponding QCD penguin and electroweak penguin are also rather suppressed.

In 2019 LHCb has announced the first observation of CP asymmetry difference between $D^0 \to K^+K^-$ and $D^0 \to \pi^+\pi^-$ with the result $\Delta A_{\rm CP} = (-1.54 \pm 0.29) \times 10^{-3}$ [30]. In the standard-model estimate with the short-distance penguin contribution, we have the expression (see e.g. [31])

$$\Delta A_{\rm CP} \approx -1.3 \times 10^{-3} \left(\left| \frac{P}{T+E} \right|_{KK} \sin\theta_{KK} + \left| \frac{P}{T+E} \right|_{\pi\pi} \sin\theta_{\pi\pi} \right), \tag{29}$$

where the factor of -1.3×10^{-3} comes from the imaginary part $2{\rm Im}(\lambda_d\lambda_b^*)/|\lambda_d|^2$, θ_{KK} is the strong phase of $(P/T)_{KK}$ and likewise for $\theta_{\pi\pi}$. Since $|P/T|$ is naïvely expected to be of order

$(\alpha_s(\mu_c)/\pi) \sim O(0.1)$, it appears that $\Delta A_{\rm CP}$ is most likely of order 10^{-4} assuming strong phases close to 90° or even less for realistic strong phases. It was pointed out in [31] that there is a resonant-like final-state rescattering which has the same topology as the QCD-penguin. That is, the penguin topology receives sizable long-distance contributions through final-state interactions. In 2012 an ansatz that $P^{\rm LD}$ is of the same order of magnitude as E was made in Ref. [31] . This ansatz of $P^{\rm LD} = E^{\rm LD} \approx E$ was justified by a recent systematical study of the final-state rescattering of the short-distance T diagram in the tolological diagrammatic approach [32]. Since the W-exchange topology can be extracted from the data, one can make a reliable prediction of $\Delta A_{\rm CP}$ as carried out in Ref. [33] in 2012, 7 years before the LHCb observation of CP violation in the charm meson sector. Hence, it is the interference between tree and long-distance penguin that pushes $\Delta A_{\rm CP}$ in the charmed meson sector up to the per mille level [33].

By the same token, CP asymmetry in the charmed baryon sector at the per mille level also can be achieved through final-state interactions as discussed recently in Ref. [34]. In particular, large CP asymmetries $\Delta A_{\rm CP}(\Xi_c^0 \to pK^-) - \Delta A_{\rm CP}(\Xi_c^0 \to \Sigma^+\pi^-) = (1.87 \pm 0.57) \times 10^{-3}$ and $\Delta A^{\alpha}_{\rm CP}(\Xi_c^0 \to pK^-) - \Delta A^{\alpha}_{\rm CP}(\Xi_c^0 \to \Sigma^+\pi^-) = (-4.94 \pm 0.57) \times 10^{-3}$ were obtained, where $\Delta A^{\alpha}_{\rm CP} = (\alpha + \bar{\alpha})/(\alpha - \bar{\alpha})$.

References

[1] H. Y. Cheng, Chin. J. Phys. **78**, 324-362 (2022).
[2] M. J. Savage and R. P. Springer, Phys. Rev. D **42**, 1527 (1990).
[3] S. M. Sheikholeslami, M. P. Khanna, and R. C. Verma, Phys. Rev. D **43**, 170 (1991); R. C. Verma and M. P. Khanna, Phys. Rev. D **53**, 3723 (1996).
[4] C. Q. Geng, C. W. Liu and T. H. Tsai, Phys. Lett. B **794**, 19-28 (2019).
[5] H. Zhong, F. Xu, Q. Wen and Y. Gu, JHEP **02**, 235 (2023).
[6] Z. P. Xing, X. G. He, F. Huang and C. Yang, Phys. Rev. D **108**, no.5, 053004 (2023).
[7] C. Q. Geng, C. W. Liu, T. H. Tsai and Y. Yu, Phys. Rev. D **99**, no.11, 114022 (2019).
[8] C. Q. Geng, C. W. Liu and T. H. Tsai, Phys. Rev. D **101**, no.5, 053002 (2020).
[9] F. Huang, Z. P. Xing and X. G. He, JHEP **03**, 143 (2022) [erratum: JHEP **09**, 087 (2022)].
[10] Y. Kohara, Phys. Rev. D **44**, 2799-2802 (1991).
[11] L. L. Chau, H. Y. Cheng and B. Tseng, Phys. Rev. D **54**, 2132 (1996).
[12] X. G. He, Y. J. Shi and W. Wang, Eur. Phys. J. C **80**, no.5, 359 (2020).
[13] Y. K. Hsiao, Y. L. Wang and H. J. Zhao, JHEP **09**, 035 (2022).
[14] H. J. Zhao, Y. L. Wang, Y. K. Hsiao and Y. Yu, JHEP **02**, 165 (2020).
[15] Y. K. Hsiao, Q. Yi, S. T. Cai and H. J. Zhao, Eur. Phys. J. C **80**, no.11, 1067 (2020).
[16] H. Y. Cheng and C. W. Chiang, Phys. Rev. D **81**, 074021 (2010); Phys. Rev. D **85**, 034036 (2012); Phys. Rev. D **86**, 014014 (2012); Phys. Rev. D **100**, 093002 (2019); Phys. Rev. D **104**, 073003 (2021).
[17] H. Y. Cheng, C. W. Chiang and A. L. Kuo, Phys. Rev. D **93**, 114010 (2016).
[18] H. Y. Cheng and C. W. Chiang, [arXiv:2401.06316 [hep-ph]].
[19] Y. Kohara, arXiv:hep-ph/9701287 [hep-ph].
[20] H. Zhong, F. Xu and H. Y. Cheng, Phys. Rev. D **109**, 114027 (2024).
[21] H. Zhong, F. Xu and H. Y. Cheng, arXiv:2401.15926 [hep-ph].
[22] J. G. Korner, Nucl. Phys. B **25**, 282-290 (1971); J. C. Pati and C. H. Woo, Phys. Rev. D **3**, 2920-2922 (1971).
[23] C. Q. Geng, C. W. Liu and T. H. Tsai, Phys. Lett. B **790**, 225-228 (2019).
[24] J. Sun, R. Zhu and Z. P. Xing, arXiv:2407.00426 [hep-ph].

[25] C. Q. Geng, X. G. He, X. N. Jin, C. W. Liu and C. Yang, Phys. Rev. D **109**, no.7, L071302 (2024).

[26] M. Ablikim *et al.* [BESIII], Phys. Rev. Lett. **132**, 031801 (2024).

[27] Yanxi Wu, talk presented at 42th International Conference on High Energy Physics, 18-24 July, 2024, Pragues, Czech Republic.

[28] S. Navas *et al.* [Particle Data Group], Phys. Rev. D **110**, 030001 (2024).

[29] Y. B. Li *et al.* [Belle], Phys. Rev. Lett. **122**, no.8, 082001 (2019).

[30] R. Aaij *et al.* [LHCb Collaboration], Phys. Rev. Lett. **122**, no.21, 211803 (2019).

[31] H. Y. Cheng and C. W. Chiang, Phys. Rev. D **85**, 034036 (2012) [arXiv:1201.0785 [hep-ph]]; **85**, 079903(E) (2012).

[32] D. Wang, JHEP **03**, 155 (2022).

[33] H. Y. Cheng and C. W. Chiang, Phys. Rev. D **86**, 014014 (2012).

[34] X. G. He and C. W. Liu, arXiv:2404.19166 [hep-ph].